Long-lived rodents reveal signatures of positive selection in genes associated with lifespan and eusociality

Arne Sahm[1*], Martin Bens[1], Karol Szafranski[1], Susanne Holtze[2], Marco Groth[1], Matthias Görlach[1], Cornelis Calkhoven[3], Christine Müller[3], Matthias Schwab[4], Hans A. Kestler[1,5], Alessandro Cellerino[1,6], Hynek Burda[7], Thomas Hildebrandt[2], Philip Dammann[7,8], Matthias Platzer[1]

[1] Leibniz Institute on Aging – Fritz Lipmann Institute, Jena, Germany.

[2] Department of Reproduction Management, Leibniz Institute for Zoo and Wildlife Research, Berlin, Germany.

[3] European Research Institute for the Biology of Ageing, University of Groningen, University Medical Centre Groningen Groningen, The Netherlands.

[4] Department of Neurology; Jena University Hospital-Friedrich Schiller University, Jena, Germany.

[5] Institute of Medical Systems Biology, Ulm University, Ulm, Germany.

[6] Laboratory of Biology Bio@SNS, Scuola Normale Superiore, Pisa, Italy.

[7] Department of General Zoology, Faculty of Biology, University of Duisburg-Essen, Essen, Germany.

[8] University Hospital, University of Duisburg-Essen, Essen, Germany.

[*] To whom correspondence should be addressed. Tel: +49 3641 656050; Fax: +49 3641 656255; Email: arne.sahm@leibniz-fli.de; Present Address: Arne Sahm, Genome Analysis, Leibniz Institute on Aging, Fritz Lipmann Institute, Jena, Thuringia, 07745, Germany.

Abstract

The genetic mechanisms that determine lifespan are poorly understood. Most research has been done on short lived animals and it is unclear if these insights can be transferred to long-lived mammals like humans. Some African mole-rats (Bathyergidae) have life expectancies that are multiple times higher than similar sized and phylogenetically closely related rodents. We obtained genomic and transcriptomic data from 17 rodent species and systematically scanned eleven lineages associated with the evolution of longevity and eusociality for positively selected genes (PSGs). The set of 319 PSGs contains regulators of mTOR and is enriched in functional terms associated with (i) processes that are regulated by the mTOR pathway, e.g. translation, autophagy and mitochondrial biogenesis, (ii) the immune system and (iii) antioxidant defense. Analyzing gene expression of PSGs during aging in the long-lived naked mole-rat and up-regulation in the short-lived rat, we found a pattern fitting the antagonistic pleiotropy theory of aging.

Introduction

Most of the available information about the genetic mechanisms that govern lifespan and aging were obtained by studying single-gene mutations in invertebrates or short-lived, highly inbred vertebrate species. However, it is not clear whether insights about aging relevant genes and pathways gained from these species can be applied to long-lived species like human [1]. In addition, lifespan extensions under artificial laboratory conditions resulting from single gene mutations or other genetic, pharmacologic and/or lifestyle interventions are far smaller than natural variation of lifespan among species shaped by natural selection. Moreover, it is not clear to what extent genetic variation is responsible for intraspecific heritable differences in lifespan overlaps with the genetic architecture of lifespan macroevolution. As a case in point, maximum lifespan in captivity varies about two orders of magnitude and is positively correlated with body mass in vertebrates [2,3], but the two traits are negatively correlated within species, the most extreme example being dog breeds [4]. Therefore,

44 comparative evolutionary approaches that search for genetic differences between closely related
45 species that are short- and long-lived with respect to their body mass may reveal novel candidate
46 genes and pathways or open new perspectives on known ones.

47 Rodents are an ideal taxon for such an approach. While the majority of species is short-lived, such as
48 mice, rats and hamsters, there are long-lived exceptions, such as chinchillas, blind mole rats (BMR,
49 *Spalax* sp.) and several African mole-rat species including the naked mole-rat (NMR, *Heterocephalus*
50 *glaber*) [5,6]. Furthermore, genome and transcriptome sequences of short- and long-lived species are
51 available and can be used for comparative analysis.

52 African mole-rats (family Bathyergidae) are subterranean rodents that feed from roots and tubers.
53 The family comprises six genera; for five out of these, maximum lifespan records are available for at
54 least one species. Notably, and in contrast to most other rodents, none of these species has a
55 maximum lifespan of below ten years or below the predictions of the power-law that describes body
56 mass/lifespan relationships in mammals [6]. At the extreme of this distribution, Zambian mole-rats
57 from the *Fukomys micklemi* clade [7] (the best studied representative being the Ansell´s mole-rat *F.*
58 *anselli*, AMR), the giant mole-rat (GMR, *Fukomys mechowii*) and NMR, have maximum lifespans of at
59 least ca. 20, 22 and 31 years, respectively. These values are 212%, 194% and 368% with respect to
60 the predicted lifespan based on their body mass ([5], GMR percentage calculated with own lifespan
61 data and same formula). In contrast, the established biomedical model organisms rat (*Rattus*
62 *norvegicus*) and mouse (*Mus musculus*) have a maximum lifespan of 3.8 and 4 years, respectively,
63 which is 32% and 51% of the predicted value. Remarkably, the greater cane rat (*Thryonomys*
64 *swinderianus*) that is closely related to the African mole-rats reaches only 28% of the predicted
65 maximum lifespan [5] (Fig. 1).

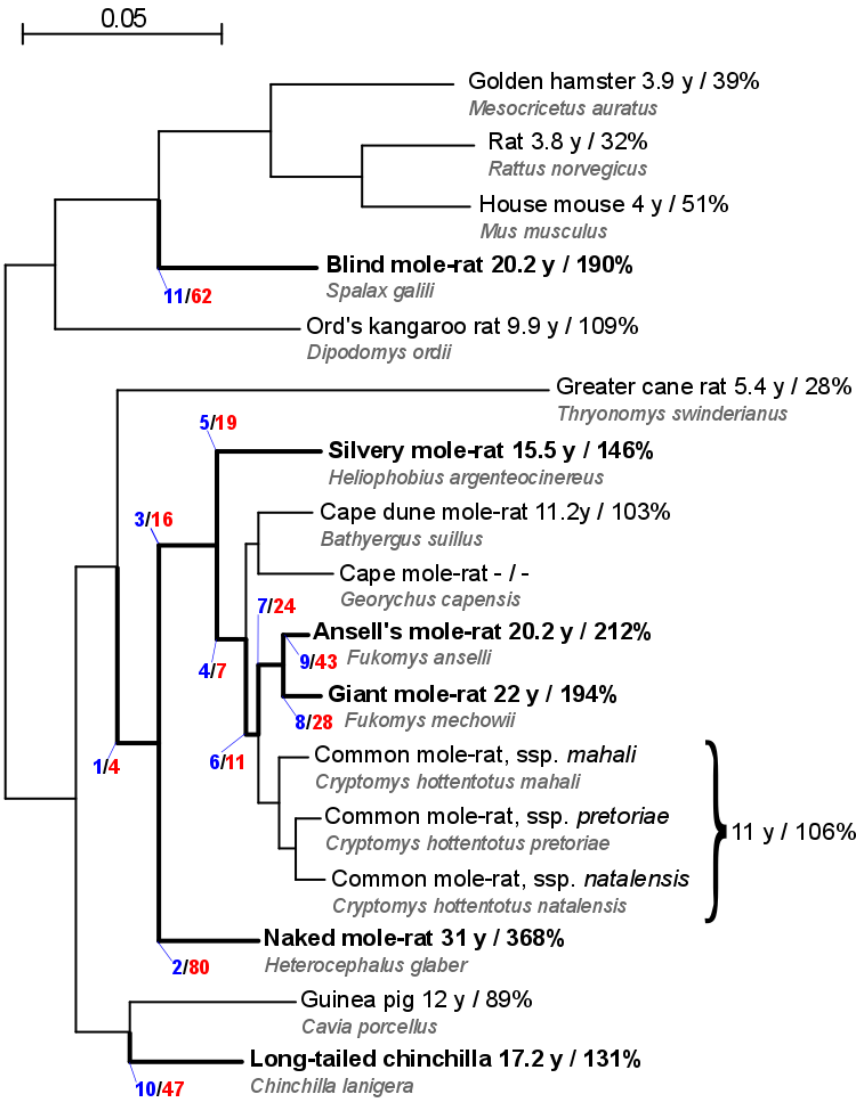

Figure 1. Nucleotide-based phylogeny of the analyzed rodents. Species or branches regarded in the present analyses as long-lived or leading to longevity, respectively, are depicted in bold. The branch numbers used in the text are shown in blue. The numbers of genes with signs of positive selection on the branches are colored in red. The first number after the species name shows the recorded maximum lifespan and the second number is the percentage of the observed vs. expected maximum lifespan based on the respective body mass. The maximum lifespans and ratios were taken from [5], except for silvery mole-rat (personal communication by R. Sumbera) and giant mole rat (own data). For these two species, the expected maximum lifespans were calculated with the same mammalian allometric equation used by [5]. The scale bar represents 0.05 substitutions per site.

78 Due to a number of unique phenotypes, the NMR became the focus of intensive research [8]. It was
79 the first vertebrate for which eusociality was discovered ([9]). The NMR shows (i) the longest lifespan
80 among rodents, (ii) no aging-related decline in reproductive and physiological parameters, as well as
81 (iii) no observable aging-related increase in mortality rate [10]. Among thousands of examined animals
82 only six recently discovered cases of spontaneous tumors have been described [11,12]. Interestingly,
83 cancer resistance is shared with BMR, which is also long-lived but, despite its name, rather distantly
84 related to African mole-rats (Fig. 1). However, different mechanisms are proposed for cancer
85 resistance in these two taxa. While high-mass hyaluronan mediated early contact inhibition was
86 suggested as a key player in NMR [13], a concerted necrotic cell death mechanism in response to
87 hyperproliferation was proposed for BMR [14].

88 The search for signatures of positive selection represents a powerful approach to identify the genetic
89 basis of these unique biological features. Positive selection is the fixation of an allele in a taxon
90 driven by its positive effect on fitness. Once an adaptive phenotype evolved in a given species or
91 evolutionary clade, some of the genes under positive selection likely play a role in it. In protein-
92 coding sequences (CDSs), positive selection results in an increased rate of non-synonymous
93 substitutions as compared to genetic drift. Statistical models based on the ratio of non-synonymous
94 to synonymous substitution rates (d_N/d_S) are widely used in comparative genomics and allow the
95 identification of specific amino acids within a given gene that changed due to positive selection [15-17]

96 Consequently, several studies performed genome-scale scans for positively selected genes (PSGs) in
97 African mole-rats and BMR. The first study [18] searched for PSGs on the very long NMR branch in a
98 four-species [19] comparison with human as an outgroup and the mouse and rat as further rodents.
99 Among the 142 identified PSG candidates, three were members of a five-protein complex involved in
100 alternative lengthening of the telomeres. The second study [20], used ten species with the guinea pig
101 (*Cavia porcellus*) as most closely related species and scanned for PSGs along the branches leading to
102 NMR, Damaraland mole-rat (*Fukomys damarensis*) and their last common ancestor (LCA), identifying
103 334, 179 and 82 candidates, respectively, including candidates associated with neurotransmission of

104 pain in the NMR. A third study [21] used species from all six African mole-rat genera and searched the
105 branch of the LCA of all African mole-rats that follows divergence from the guinea pig. Signs of
106 positive selection were identified in 513 genes, including loci associated with tumorigenesis, aging,
107 morphological development and sociality. All three studies suffer from a methodological limitation
108 that is common in positive selection studies: in none of these, a closer related species than guinea
109 pig was included. As guinea pig is not the closest relative of African mole rats not expressing the
110 phenotypes of interest, it cannot be excluded that fixation of detected signs of positive selection
111 predates – and therefore could not contribute to – the evolution of these phenotypes [22]. A fourth
112 study [23] examined the BMR branch using the Chinese hamster (*Cricetulus griseus*) as the most closely
113 related outgroup. Among the 48 PSG candidates, several were linked to necrosis, inflammation and
114 cancer.

115 To better resolve the above-mentioned ambiguities and to achieve a higher resolution of positive
116 selection along rodent phylogenetic branches leading to longevity and eusociality, we analyzed
117 genomic and transcriptomic data of 17 species – data from public sources and original data
118 generated for this study. In particular, we generated genomic data for the greater cane rat as a key
119 species absent from previous analysis and for the silvery mole-rat (SMR, *Heliophobius*
120 *argenteocinereus*). We systematically scanned 11 evolutionary branches (6 corresponding to extant
121 species and 5 to ancestral branches). This approach enables us to date precisely the occurrence of
122 signatures of positive selection with respect to the evolution of the phenotypes of interest on
123 multiple evolutionary branches of rodents. In addition, we generated RNA-seq data from young and
124 old NMRs and laboratory rats (*Rattus norvegicus*) to analyze the overlap between PSGs and genes
125 regulated during aging. Based on this, we discuss the implications of these results on our
126 understanding of the genetic basis of aging, lifespan and sociality.

127

Results and Discussion

As starting points for our analysis, we generated CDS libraries for five rodent species (NMR, AMR, GMR, SMR and greater cane rat) based on transcriptomic and genomic data. (Table S1/S2). Together with publicly available rodent CDS catalogs (Table S1), we obtained data for 17 species, including several additional African mole-rats, the chinchilla, BMR and short-lived outgroups like the guinea pig, mouse and rat (Fig. 1). From these sequences, we predicted orthologs and best matching isoforms between the species, calculated alignments and applied multiple times the branch-site test of positive selection [24].

Based on the lifespans of the extant species, we regarded six extant as well as five ancestral branches as leading to enhanced longevity and examined them for positive selection (Fig. 1). In total, we detected 341 PSGs ($p<0.05$, branch-site test). Our PSG assignment is based on nominal p-values, a common approach in genome-wide scans [21,25,26] since the main error source of such analyses are alignment errors [27] which result in extremely small p-values and therefore cannot be controlled by multiple test corrections. Furthermore, simulations have shown that the empirical false positive rate is very low if an appropriate filtering is used to remove alignment errors and unreliable results [28].

Twenty genes were found on multiple branches (Table S3), resulting in a non-redundant set of 319 PSGs (Table S4-S15). Signs of positive selection for the same gene on multiple branches indicate possible parallel evolution. Among those, we found *AMHR2* (anti-Mullerian hormone receptor type 2) to be positively selected both on branch 2 (NMR) and branch 11 (BMR). While AMHR2 plays a role in male fetal development and in ovarian follicle development of the adult female [29], no function with regard to aging is described yet. However, the protein kinase domain of AMHR2 contains the greatest number of longevity-selected positions based on a regression analysis with 33 mammalian species [30]. This domain contains 3 of 8 and 2 of 3 positively selected sites on branch 2 (NMR) and branch 11 (BMR), respectively.

153 **Different studies on positive selection in mole-rats show minor overlaps**

154 First, we compared our list of PSGs with the PSGs detected in previous studies of positive selection in
155 mole-rats [18,20,21,23] (Table S16). As observed before, [21] PSGs from different studies show no or small
156 overlaps. This is not surprising because the branches examined in previous studies represent
157 different phylogenetic entities than those used here, even though some of them are named similarly.
158 For example, Kim et al. examined an "NMR branch" using the house mouse as closest related species
159 [18]. In our study, the sister taxon to NMR is represented by other African mole-rats and the house
160 mouse is used only as an outgroup (Fig. 1). In a similar way, the analysis of the African mole-rat
161 ancestor by previous studies [21,23] differs from ours as we incorporated the greater cane rat as closest
162 related short-lived species and used guinea pig as an outgroup. We therefore analyzed evolutionary
163 processes on a shorter phylogenetic distance that closely matches the appearance of the phenotypes
164 under investigation. In addition, there are methodological differences between the studies, e.g.
165 regarding ortholog prediction or alignment filtering. Unfortunately, the contribution of these
166 technical variables to the discrepancies cannot be assessed as the alignments used for the previous
167 studies are not available and cannot be compared with those generated and provided in our study
168 (Supplement Data).

169

170 **Positive selection and age-related regulation are linked**

171 Next, we analyzed the direction of the regulation of PSGs during aging to identify potential links
172 between positive selection on the analyzed branches and genetic determinants of lifespan. In
173 general, directionality analysis of gene regulation during aging is complicated by the fact that the
174 direction itself is not informative, whether the respective gene function is either causing or
175 counteracting aging. E.g. up-regulation of a causative gene may accelerate aging and shorten lifespan
176 while adaptive up-regulation to counteract aging phenotypes may extend longevity. We recently
177 observed that PSGs in short-lived and fast-growing killifish were significantly more often up- than

down-regulated during aging [17]. This finding is consistent with the concept of antagonistic pleiotropy [31] suggesting that the same genes that are positively selected in short-lived species for fast growth and maturation at young age are drivers of aging at old age. The antagonistic pleiotropy hypothesis is well supported, e.g. by the fact that growth rate and lifespan are negatively correlated, both between species and within many species [6,32]. If, however, up-regulation of PSGs in short-lived species may cause aging, we hypothesized that selection for longevity is more compatible with attenuation of gene activity – either on the level of protein function or gene regulation – since avoiding damage is easier than improving repair.

Following this hypothesis, we performed RNA-seq in liver from old vs. young males of both long-lived NMRs and short-lived rats (>21 vs. 2-4 years and 24 vs. 6 months, respectively; Table S17-S19). Indeed, the union of PSGs showed preference for down-regulation in NMR and for up-regulation in rats in respect to all regulated genes (p=0.0089, Lancaster procedure [33]). Moreover, the down-regulation in the long-lived and up-regulation in the short-lived species originate largely from the same genes as in a combined view on aging related expression changes in NMR and rat (Fig. 2), PSGs showed a highly significant preference for quadrant I (down in NMR, up in rat; p=0.0014, one-sided fisher test, quadrant I against the sum of II, III, IV). These results indicate that identified PSGs are associated with expression changes during aging of long- and short-lived rodents consistent with the antagonistic pleiotropy theory of aging.

To functionally annotate PSGs in respect to aging, we performed gene ontology (GO) term enrichment analysis. Regarding all genes, there was a significant enrichment for down-regulation in 126 terms during NMR aging while no term was enriched for up-regulation (Table S20, FDR<0.05, GAGE). The enriched 126 terms were summarized into 16 categories (Tables S21/S22, REVIGO). Among the six top categories are “translation” (GO:0006412), “cellular respiration” (GO:0045333), “response to oxidative stress” (GO:0006979) and “iron ion homeostasis” (GO:0055072) previously linked to aging (see below). With respect to possible pleiotropic effects, translation and cellular respiration are also key components of the growth program. To evaluate the PSGs in respect to these

204 categories, we built the union of genes for each category and tested for overrepresentation of PSGs.
205 Regarding all PSGs, there was a significant overlap with "cellular respiration" (p=0.0022, one-sided
206 fisher test) and "response to oxidative stress" (p=0.029). Regarding only the 82 PSGs that were down-
207 regulated in NMR and up-regulated during rat aging (quadrant I, Fig. 2), all four categories were
208 significantly enriched (cellular respiration: $p=2.1*10^{-6}$, response to oxidative stress: p=0.022, iron ion
209 homeostasis: $p=8.5*10^{-4}$, translation: p=0.011; Table S23). This again suggests that PSGs are linked to
210 aging relevant processes in an antagonistic pleiotropic way. The result is also consistent with the
211 hyperfunction theory of aging that suggests that antagonistic pleiotropy works via a mechanism of
212 "perverted" growth. According to this theory the growth program that is beneficial during youth is
213 not entirely stopped after finishing development and causes damage from that point on. The theory
214 further claims that the master regulator mTOR governs this growth program [34,35].

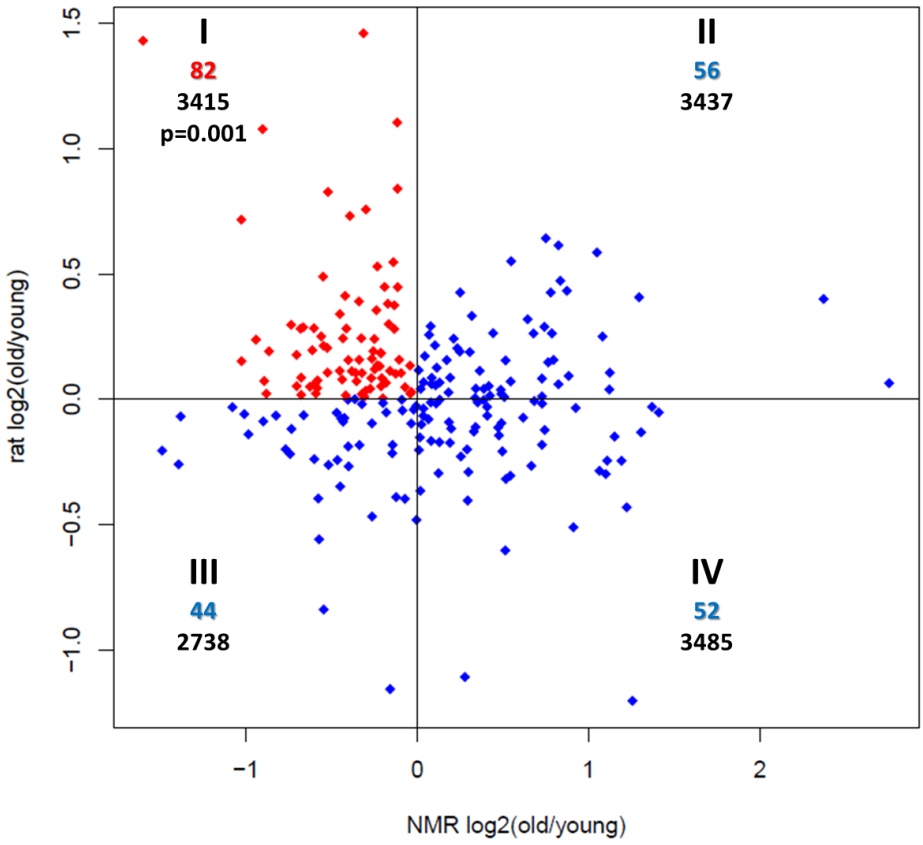

215

216 **Figure 2.** PSG expression changes during aging of NMR and laboratory rat. The roman numbers
217 describe the quadrant, the colored numbers below that show the number of PSGs in the respective
218 quadrant and the black numbers at the bottom give the total regulated genes in the quadrant. The

219 red marked quadrant (I) represents PSGs that were down regulated in the long-lived NMR and up
220 regulated in the short-lived rat and tested against the sum of three blue marked quadrants (II, III, IV)
221 with Fisher's exact test (one-sided). The resulting p-value is shown in quadrant I. The total number of
222 PSGs shown in this plot (234) is lower than the unique number of all PSGs (319) due to missing
223 expression of genes in NMR and/or rat as well as missing log2-fold-changes in at least one of the
224 species (DEseq2).

225

226 **Inflammation and host defense are enriched in branches leading to longevity**

227 Subsequently, we searched for enriched gene ontologies in the union of PSGs across the 11 branches
228 along which longevity evolved and in each of these branches separately (Table S24). We found
229 enrichments of genes involved in inflammatory response (GO:0006954; FDR=0.0068, Fisher's exact
230 test) and defense response (GO:0006952, FDR=0.0092). Aging is tightly associated to the delicate
231 balance between pro-inflammatory responses to resist potentially fatal infections and the inexorable
232 damages that are accumulated by this [36,37]. Chronic inflammation is described as a major risk factor
233 for aging and aging-related diseases such as atherosclerosis, diabetes, Alzheimer's disease,
234 sarcopenia and cancer [38].

235

236 **mTOR, autophagy and translation pathways show signs of positive selection leading to longevity**

237 On branch 2 (NMR), we found *RHEB* (Ras homolog enriched in brain) coding for a direct regulator of
238 mTOR (mechanistic target of rapamycin) and on branch 9 (AMR) its paralog *RHEBL1* to be positively
239 selected, a situation consistent with the concepts of parallel evolution as well as of
240 subfunctionalization of genes after duplication. mTOR operates as a central regulator of cell
241 metabolism, growth, inflammation and proliferation and was identified as a key regulator of aging
242 and aging-related diseases in yeast, nematodes, fruit flies, and mice [39,40].

mTOR is also a key regulator of autophagy [41]. Autophagy is a cellular protective cleaning mechanism, required for organelle homeostasis, especially mitochondria. While enhanced autophagy was shown to be associated with lifespan extension in worms, flies and mice, inhibition of autophagy, conversely, leads to premature aging in mice [42]. An essential autophagy gene, *LAMP2* (lysosomal associated membrane protein 2), was identified as PSG on branch 2 (NMR) and branch 11 (BMR). As a receptor for chaperone-mediated autophagy and a major protein component of the lysosomal membrane, LAMP2 is required for degradation of individual proteins through direct import into the lysosomal lumen [43,44]. Aging-dependent decrease of *LAMP2* expression was observed in mouse liver. Reinstatement of juvenile LAMP2 levels in aged mice significantly reduces aging-dependent decline of cell function and restores the degree of cell damage to that found in young mice [45].

Besides the lysosome, another cellular protein quality control and degradation system is the proteasome. While impaired proteasome function and subsequent accumulation of misfolded proteins were tightly correlated with aging and aging-related neurodegenerative disorders like Parkinson's and Alzheimer's disease, long-lived humans have sustained proteasome activity [46-48]. Two proteasome subunit genes, *PSMG1* (proteasome assembly chaperone 1) and *PSMB4* (proteasome subunit beta 4), were identified as PSGs on branch 11 (BMR). PSMB4 has been classified as a driver for several types of tumors [49] and is a known interaction partner of PRP19 (pre-mRNA-processing factor 19 or senescence evasion factor) that is essential for cell survival and DNA repair [50].

Another aging relevant downstream process regulated by mTOR is translation. We identified two ribosomal proteins, RPL7L1 and RPL27A, on branch 3 (LCA of all African mole-rats except NMR). While in general, cytosolic ribosomal proteins are up-regulated with aging in humans [51], rats [52] and killifish [53] both genes are significantly down-regulated during NMR aging (FDR≤0.05, DESeq2). This fits the down-regulation of translation-related processes during NMR aging in general (see above). Furthermore, the protein synthesis machinery is a driver of replicative senescence in yeast [54]. The longitudinal aging study in killifish [55] highlighted the starting values at 10 weeks and the amplitude of age-dependent increase of ribosomal proteins to be negatively correlated with lifespan. Inhibition of

protein synthesis by reduction of ribosomal proteins was shown to extend lifespan in worms [56] and mice [57].

Positive selection leading to longevity affects mitochondrial biogenesis and regulation of oxidative stress

Besides regulation of cytoplasmic translation of nuclear encoded genes, mTOR is also involved in mitochondrial translation. There appears to be a complex interplay between mTOR signaling, mitochondrial gene expression and oxygen consumption as well as production of reactive oxygen species (ROS) [58-60]. Across multiple longevity-associated branches we identified PSGs that are involved in mitochondrial biogenesis (Table 1). We found, e.g., an enrichment of "mitochondrial translation" (GO:0032543, FDR=0.044) on branch 5 (SMR), the mitochondrial transcriptional termination factor (MTERF) on branch 2 (NMR) and six mitochondrial ribosomal proteins (MRPs) distributed on branches 5 (SMR), 7 (LCA of AMR and GMR) and 11 (BMR). Furthermore, nuclear encoded genes of respiratory chain complex I (*NDUFA9* and *NDUFB11*: NADH ubiquinone oxidoreductase subunits A9 and B11) and complex IV (*COX14*: cytochrome c oxidase assembly factor COX14) were identified as PSGs. Of note, we found 6 of these 15 genes to be significantly down-regulated during aging in NMR (Table 1). This suggests a functional relation of these genes to the aging process in an extremely long-lived rodent and is concordant with the down-regulation of genes involved in cellular respiration during NMR aging described above.

289 **Table 1.** Mitochondrial biogenesis genes under positive selection on longevity-associated branches.

Gene	Positively selected on branch		NMR aging	Function in mitochondrium
	Branch number	Branch description		
NDUFA9	8	GMR	↓	Complex I
MTERF	2	NMR	ns	Transcription
SDHAF2	2	NMR	ns	Complex I
UQCRC2	2 3	NMR LCA after NMR divergence	↓	Complex III
NDUFB11	5	SMR	↓	Complex I
MRPS11	5	SMR	↓	Translation
MRPS36	5	SMR	↓	Translation
MRPL30	5	SMR	↓	Translation
TRNT1	11	BMR	ns	RNA processing
COX14	11	BMR	ns	Complex IV
DARS2	11	BMR	ns	RNA processing
MRPL57	11	BMR	ns	Translation
MRPL15	11	BMR	ns	Translation
MRPL28	7	Fukomys LCA	ns	Translation
GATC	10	long-tailed chinchilla	ns	RNA processing

290 Note: Branch numbers refer to figure 1. LCA – last common ancestor; ↓– significantly lower
291 expressed in liver of old animals compared to young animals (FDR<0.05); ns – not significantly
292 changed.
293

294 Studies in mouse and the short-lived killifish have shown that expression of MRPs and complex I
295 genes is negatively correlated with individual lifespan [55,61]. Knock-down of MRPs in worms results in
296 an impaired assembly of respiratory complexes and life-extension [62]. Furthermore, we recently
297 identified a significant enrichment of mitochondrial biogenesis genes including those for multiple
298 MRPs, complex I components and MTERF among PSGs on two ancestral branches of annual killifishes
299 on which lifespan was shortened considerably and independently from each other [17]. Altogether,
300 these results raise again the intriguing possibility that similar or even the same genes could be
301 causally linked to the evolution of both short and long lifespan.

302 Mitochondria are also the main source of ROS that cause oxidative stress, i.e. damages to DNA,
303 proteins and other cellular components [63]. Oxidative stress is thought to play a major role in the
304 pathogenesis of neurodegenerative diseases [64] and even the determination of lifespan in general
305 ("oxidative stress theory of aging") [65]. On branch 3 (LCA of all African mole-rats except NMR), we

306 found an enrichment of oxidoreductase activity (GO: GO:0016491; FDR=0.024) and positive selection
307 of *TXN* (thioredoxin), coding for an oxidoreductase enzyme that acts as an antioxidant extending
308 lifespan in fly [66] and potentially also in mice [67,68]. As an example of continued evolution, *TXN* was
309 found to be positively selected also on branch 7 (LCA of AMR and GMR). *SOD2* (superoxide dismutase
310 2) and *CCS* (copper chaperone for superoxide dismutase) are PSGs on branch 10 (chinchilla) and
311 branch 2 (NMR), respectively. Both genes are involved in ROS defense and affect aging/lifespan in
312 several species [69,70]. This is interesting because in recent years, it has been repeatedly questioned
313 that the oxidative stress theory of aging has much relevance for bathyergid rodents, given that
314 several studies failed to find improved antioxidant capacities and/or less accumulation of oxidative
315 damage in NMRs compared to the much shorter-lived mice [71-73]. This is consistent with our finding of
316 down-regulation of processes involved in "response to oxidative stress" (GO:0006979) during aging in
317 NMR (see above). On the other hand, significantly higher levels of oxidative damage on proteins and
318 lipids in non-reproductive as compared to reproductive females of the Damaraland mole-rat were
319 found [74]. Since non-reproductive individuals live shorter (and hence age faster) than their
320 reproductive counterparts in *Fukomys* sp. [75-77], these results are consistent with the oxidative stress
321 theory of aging. The diverse signs of positive selection on branch 2 (NMR), 3 (LCA of all African mole-
322 rats except NMR) and 7 (LCA of AMR and GMR) may suggest that the impact of oxidative stress on
323 aging differs between NMR and other African mole-rats.

324 ROS production and ROS-induced damage to biomolecules are intertwined with the formation of
325 advanced glycation end-products (AGEs). AGEs are stable bonds between carbohydrates and
326 proteins/lipids which are formed in a non-enzymatic fashion. AGEs activate membrane-bound or
327 soluble AGER (AGE specific receptor) and AGEs/AGER have been linked to several aging-related
328 diseases including Alzheimer's disease and diabetes [78]. Interestingly, *AGER* was found to be a PSG on
329 branch 9 (AMR) and branch 10 (chinchilla). The role of AGEs/AGER in aging is complex and Janus-
330 faced [79]. AGER is significantly up-regulated in liver during NMR aging. Similarly, in skin AGE levels rise

with chronological age in AMR, but surprisingly are higher in the skin of slow aging breeders than of faster aging non-breeders [80]

Additional links between positive selection and longevity

The gene *APOA1* (apolipoprotein A1) was found as PSG on branch 7 (LCA of AMR and GMR) and significantly up-regulated during NMR aging in liver. APOA1 is a component of HDL-particles which are as transporter of cholesterol relevant for aging-associated diseases. Polymorphisms of APOA1 are associated to coronary artery disease [81]. Furthermore, APOA1 is an interaction partner of APOE a well-described genetic risk factor for Alzheimer's and cardiovascular diseases [82] and the locus with the largest statistical support for an association with extreme longevity [83]. Same as *MTERF* (see above), *APOA1* is one of nine genes that we recently found to be positively selected on both of two ancestral sister branches of annual fishes on which lifespan was independently reduced [17].

TF (transferrin) was identified as PSG on branch 4 (LCA of Cape, Cape dune, giant, AMR and common mole-rats). TF is an iron-binding protein responsible for transport of iron in the bloodstream and therefore essential for iron homeostasis [84]. Neurons regulate iron intake via the TF receptor and dysregulation of this tightly controlled process in the brain is associated with neurodegenerative, age-related diseases like Parkinson's and Alzheimer's [85]. TF is significantly down-regulated during NMR aging which is consistent with the down-regulation of "iron ion homeostasis" (GO:0055072) related processes during NMR aging in general (see above).

Selection signatures of social evolution among African mole rats is consistent with a scenario of ancestral eusociality

Although all African mole-rats are strictly subterranean and occupy similar nutritional niches, intra-familiar variety of social and mating systems is amazingly high. Solitariness and polygamy in some

355 genera (*Heliophobius*, *Georychus* and *Bathyergus*) contrast sharply with social organization in others
356 (*Heterocephalus*, *Fukomys* and *Cryptomys*). In the latter, stable monogamous bonding of (typically
357 one) reproductive founder pair coupled with prolonged philopatry and reproductive altruism of their
358 offspring result in extended and cooperatively breeding family units, which can grow to considerable
359 size. There has been much debate whether eusociality in African mole-rats is a derived or ancestral
360 trait [86,87]. The first scenario assumes a solitary LCA of African mole-rats (branch 1) and subsequent
361 independent, parallel evolution of eusocial habits on branch 2 (NMR) and branch 6 (LCA of AMR,
362 GMR and common mole-rats) and/or branch 7 (LCA of AMR and GMR) [21]. In contrast, the second
363 scenario suggests a eusocial LCA of all mole-rats (branch 1) and independent loss of this phenotype in
364 the SMR (branch 5) and the LCA of the genera *Bathyergus* and *Georychus* (Cape and Cape dune mole-
365 rat). Recent phylogenetic approaches are more supportive of scenario 2 [88,89] however, a PSG-based
366 analysis of the issue is still lacking. Accordingly, we searched our data in support of one or the other
367 scenario.

368 All four PSGs found on the ancestral branch 1 of all African mole-rats are involved in signaling,
369 resulting in enrichments, e.g., of "positive regulation of cell communication" (GO:0010647,
370 FDR=0.0092) and "positive regulation of signaling" (GO:0023056, FDR=0.0092). Enrichments in signal
371 transduction were identified as major common pattern of the multiple independent occurrences of
372 eusociality in bees [90] strongly suggesting parallel evolution in eusocial insects and mammals.

373 On the other hand, members of the major histocompatibility complex (MHC) were identified as PSG
374 on branch 2 (NMR) and on branch 7 (LCA of AMR and GMR). MHC genes have a central function in
375 the acquired immune system and immune dysfunction is involved in many neurodevelopmental
376 disorders as well as social behavior deficits in mice and humans [91,92]. MHCs have been implicated in
377 language impairment and schizophrenia [93,94]. A human allele of *HLA-A* was associated with autism
378 defined as a pattern of behavior identified by deficits in communication and reciprocal social
379 interactions [95].

Additionally, we found two signals with a potential link to social evolution on branch 2 (NMR), but not branch 6 (LCA of AMR, GMR and common mole-rats) or 7 (LCA of AMR and GMR). The first were innate immune system related enrichments "positive regulation of T cell activation" (GO:0050870, FDR=0.027) and "positive regulation of leukocyte cell-cell adhesion" (GO:1903039, FDR=0.027). In social ants and bees, it was shown that several innate immune genes have a pattern of accelerated amino acid evolution compared both to non-immunity genes in the same species and immune genes in solitary fly [96]. Second, we found *NOTCH2* positively selected only on branch 2 (NMR). The encoded protein is one of four Notch-receptors. Notch signaling regulates interactions between physically adjacent cells and has a central role in the development of many tissues, including neurons [97]. It was demonstrated that Notch signaling represses reproduction in worker honeybees depending on the presence of the queen and that chemical inhibition of Notch signaling can overcome the repressive effect of queen pheromone in regard to the worker ovary activity [98].

On the other hand, *HSD11B1* (hydroxysteroid 11-beta dehydrogenase 1) was identified as PSG on branch 6 (LCA of AMR, GMR and common mole-rats), but not branch 2 (NMR). The encoded protein catalyzes reversibly the conversion of the stress hormone cortisol to the inactive metabolite cortisone [99]. Cortisol concentration was shown to inversely correlate with social ranks in NMRs [100] and with anti-social and isolation behavior in human adolescents [101,102]. Furthermore, cortisol regulates carbohydrate metabolism that is another common enriched GO-Term in the evolution of eusociality in bees [90]. Not linked to eusociality but still noteworthy, *HSD11B1* is significantly down-regulated during aging in the NMR and knockout of *HSD11B1* in mice improves their cognitive performance in aging [103]. Furthermore, inhibition was described as a risk factor for cardiovascular disease and diabetes type 2 [104].

Taken together, our data are on best agreement with a scenario assuming eusociality (or a predisposition for it) in the LCA of all African mole-rats, followed by further independent, branch-specific evolution or loss of the phenotype leading to the distinct social genera that live today.

405

406 **Homology modeling suggests functional consequences of amino acid changes under positive**
407 **selection**

408 To evaluate the structural impact of positively selected amino acid changes, we performed homology
409 modeling using exemplary the sites of highest probability for selection in cytoplasmic thioredoxin
410 (TXN) and transferrin (TF). As mentioned above *TXN* is positively selected on branch 7 (LCA of AMR
411 and GMR). In TXN of these species, there is a tyrosine residue that replaces Cys69. The latter,
412 together with Cys62 and Cys73, constitute highly conserved mammalian non-catalytic cysteines. The
413 local structure around Cys69 and Cys62 in TXN is important for interaction with the cytoplasmic
414 thioredoxin reductase (TR1; [105]), which 'recycles', i.e. re-reduces, the catalytic cysteines of oxidized
415 TXN. The modeling using the structure of a fully reduced human TXN (1ERT*;* [106]) as template suggests
416 that the rather bulky side chain of Tyr69 can be accommodated in the structure of TXN (Fig. 3A),
417 hence allowing for a productive helical interface region to TR1. TXN recycling is inhibited by
418 formation of a disulfide bridge between Cys62 and Cys69 (Fig S1; see [107]), e.g. under highly oxidative
419 conditions, thereby diminishing the pool of catalytically active TXN under oxidative stress [108,109].
420 Obviously, that disulfide bridge cannot form in AMR and GMR because of Cys69Tyr. From this, we
421 conclude that Tyr69 is compatible with TXN recycling also under oxidative stress. Moreover, Cys69 is
422 known to be a target for posttranslational modifications with impact on e.g. anti-apoptotic/apoptotic
423 signaling pathways (for a review see: [110]), raising interesting questions on physiological consequences
424 of the Cys69Tyr replacement.

425
426 **Figure 3**. Homology models of Ansell's mole-rat (AMR) thioredoxin (TXN) and transferrin (TF). (A)
427 Overview of the modeled AMR TXN structure (green) superimposed onto the fully reduced human
428 TXN template structure (1ERT, grey). Residues discussed in the text are labeled, numbering according
429 to position in the human sequence. Color code of Cys69 and Tyr69 corresponds to the respective
430 ribbon representation. Heteroatoms: sulfur in yellow, oxygen in red. (B) Overview of the modeled
431 AMR TF structure (green) superimposed onto the rabbit TF template structure (1JNF, grey). The
432 position of the Asn383Lys site discussed in the text at the boxed center of the lobe interface
433 numbered and indicated in cyan. Brown spheres: Fe^{3+} coordinated in the template structure (1JNF,
434 ion radius enlarged for better visibility). (C) Detail of the TF lobe interface. Shown is a magnification
435 of the boxed region in (B). Coloring and numbering as in (B), side chain nitrogen atoms (blue), oxygen
436 atoms (red). Potential hydrogen bond in 1JNF (light blue) as discussed in the text. Numbering (black)
437 according to positions in the rabbit TF structure (1JNF).

438 TF is a PSG on branch 4 (LCA of Cape, Cape dune, giant, AMR and common mole-rats) and Ser383Lys
439 is the site of highest probability for selection. Serum TFs form a bilobal structure, and each lobe
440 contains two dissimilar domains with a single iron-binding site. Inspecting the structure of the AMR
441 TF modeled on the rabbit protein (1JNF; [111]) as template, we realized that Lys 383 is located at the
442 interface between the two lobes (Fig. 3B). In the rabbit TF two juxtapositioned Asn residues at
443 position 383 and 312 might form an H-bond and this constellation could stabilize the inter-lobe
444 interactions (Fig. 3C). In contrast, the juxtaposition of the positively charged side chains of Lys383
445 and a conserved Arg312 in the AMR structural model (Fig. 3C) would be expected to weaken the

446 lobe-lobe interaction due to electrostatic repulsion. The functional consequences for TF or TXN
447 implied by this modeling require experimental validation.

448 Conclusions

449 We provided a systematic scan for PSGs on evolutionary branches of the African mole-rat family and
450 other rodents leading to longevity and eusociality. Due to the incorporation of species from all six
451 genera of the African mole-rats as well as its closest relative, the cane rat, into the analysis, we were
452 able to examine considerably more extant and ancestral branches than previous studies. This
453 enabled the analysis to provide a high resolution of positive selection on branches on which the
454 mentioned traits had evolved.

455 Analyzing the gene expression of PSGs, we found a highly significant pattern of down-regulation in
456 the long-lived NMR and up-regulation in the short-lived rat, fitting the antagonistic pleiotropy theory
457 of aging [112] and the hyperfunction theory of aging. The latter claims mTOR as a central hub affecting
458 aging and lifespan [35]. Correspondingly, the PSGs and enriched functional terms cover many of the
459 processes that are regulated by the mTOR pathway, e.g. translation, autophagy and mitochondrial
460 biogenesis. Furthermore, with *RHEB* and its ortholog *RHEB1L* direct regulators of mTOR [113] are under
461 positive selection in two of the branches. In addition, we linked positive selection with immune
462 system and the antioxidant defense, processes known to be involved in regulation of lifespan.

463 With regard to evolution of eusociality, our findings are in line with the theory that the LCA of all
464 African mole-rats had at least a predisposition for social lifestyle that was lost in some lineages, while
465 in other lineages the ancestral phenotype has further evolved, leading to the distinct social
466 phenotypes in the extant species.

467 Moreover, we exemplarily showed potential functional relevance of the positively selected sites by
468 homology modeling on the protein level. This may encourage experimental follow-up studies since all

sequences and alignments including the identified positively selected sites are accessible via supplement data.

Methods

CDS data

We examined nine African mole-rat species covering all six genera. Additionally, our analysis comprises eight outgroup species, including the long-lived BMR and the chinchilla. mRNA sequences of seven distantly related outgroup species were obtained from RefSeq along with their CDS annotation (Table S1). For the NMR we used a recently published *de novo* transcriptome assembly [114]. RNA-seq data for six mole-rat species was obtained from GenBank Sequence Read Archive, study SRP061925 [21]. The reads were assembled and annotated using FRAMA as described in [114].

For AMR and GMR, purification of RNA from 13 and 17 tissues, respectively, was done using Qiagen RNeasy Mini Kit following the manufacturer's description. Novel RNA-seq was performed for both species as described in Table S2. *De novo* transcriptome assemblies of the generated data were performed using FRAMA [114] (see Table S1).

For the SMR and the greater cane rat genome sequencing was performed to complement the transcriptome data. DNA was isolated from liver tissue of two female SMR individuals and a male liver of the greater cane rat using DNeasy Blood & Tissue (Qiagen). DNA was then converted to Illumina libraries and sequencing was done as given in Table S2. Sequence reads were cleaned by removal of adaptors and low-quality regions at the ends (i.e. regions with more than 10% with quality score ≤ 20). Low quality reads (i.e. less than 50% remained) and duplicons were discarded. *De novo* genome sequence assembly was performed using CLC assembler (CLC Genomics) with default settings. The CDS annotation was done using AUGUSTUS [115] with AMR CDSs as hint.

All animals were housed and euthanized compliant with national and state regulations. Read data was deposited as ENA (European Nucleotide Archive) study PRJEB20584.

Identification of positively selected genes

To scan on a genome-wide scale for genes under positive selection, we fed the CDSs of the described species set along with the branches we wanted to examine (Fig. 1) into the PosiGene pipeline [28]. GMR was used as PosiGene's anchor species. Regarding the SMR, for which we had both a genome and a transcriptome assembly, we used generally the transcriptome assembly, except for those ortholog groups in which no SMR ortholog could be assigned via transcriptomic but via genomic data. This was accomplished by calling the three PosiGene modules separately, feeding both assemblies independently in the first module (ortholog assignment) and deleting all genome-based SMR sequence in those ortholog groups that contained transcriptome-based SMR CDSs before calling the second module. An overview about the number of genes and sequences tested for positive selection in the different branches is shown in Table S1. We considered all genes with nominal p-values ≤ 0.05 as PSGs.

Gene ontologies

We determined enrichments for GO categories with Fisher's exact test based on on the R package GOstats. The resulting p-values were corrected using the Benjamini-Hochberg method (FDR).

Differentially expressed genes during NMR and rat aging

The young and old rats (strain Wistar) had an age of 6 (n=4) and 24 (n=5) months, respectively. The young NMRs had an age of 3.42±0.58 years (average±sd, n=6). The old NMRs were at least 21 years

old (recorded lifetime in captivity, n=3). All examined animals were males. All animals were housed and euthanized compliant with national and state regulations. For both species, purification of RNA from liver samples was done using Qiagen RNeasy Mini Kit following the manufacturer's description. In short, we performed RNA-seq using Illumina HiSeq 2500 with 50 nt single read technology and a sequencing depth of at least 20 mio reads/sample (Table S17). For NMR, the read mapping was performed with STAR [116] (--outFilterMismatchNoverLmax 0.06 --outFilterMatchNminOverLread 0.9 --outFilterMultimapNmax 1) against the public genome (Bioproject: PRJNA72441) that we had annotated before by aligning the above mentioned NMR transcriptome reference using BLAT [117] and SPLIGN [118]. Rat reads were aligned against the mentioned RefSeq reference using bwa aln [119] (-n 2 -o 0 -e 0 -O 1000 -E 1000). Read data and counts were deposited as GEO (Gene Expression Omnibus) series GSE98746. Differentially expressed genes (FDR≤0.05, Table S18, S19) and fold-changes were determined with DESeq2 [120]. GAGE [121] was used to determine enriched gene ontologies based on fold-changes (Table S20). Gene ontologies with FDR≤0.05 were summarized using REVIGO (allowed similarity=0.5) [122]. Four of the six largest summarized categories of the resulting treemap (Table S21/S22) were further analyzed due their aging relevance (representative terms given): “translation” (GO:0006412), “cellular respiration” (GO:0045333), “response to oxidative stress” (GO:0006979) and “iron ion homeostasis” (GO:0055072). For each of these categories the union of genes across gene ontology terms was built. These unions were tested for significant overlaps with (i) the union of PSGs across branches and (ii) the union of PSGs across branches that were down-regulated during aging in NMR and up-regulated in rat (Fisher’s exact test). Functional annotation of the PSGs in respect to the four categories is given in Table S23).

Homology modeling of protein structure

Models were built in SWISS-MODEL (http://swissmodel.expasy.org;) [123,124]. No further optimization was applied to the resulting TXN and TF models. Superimposition of the model and template structures and rendering was carried out using CHIMERA [125].

Data availability

Read data for AMR, GMR, SMR and greater cane rat was deposited as ENA (European Nucleotide Archive) study PRJEB20584. Read data for NMR and rat was deposited as GEO (Gene Expression Omnibus) series GSE98746.

References

1 Austad, S. N. Comparative biology of aging. *J Gerontol A Biol Sci Med Sci* **64**, 199-201, doi:10.1093/gerona/gln060 (2009).

2 Austad, S. N. Diverse aging rates in metazoans: targets for functional genomics. *Mech Ageing Dev* **126**, 43-49, doi:10.1016/j.mad.2004.09.022 (2005).

3 de Magalhaes, J. P., Costa, J. & Church, G. M. An analysis of the relationship between metabolism, developmental schedules, and longevity using phylogenetic independent contrasts. *J Gerontol A Biol Sci Med Sci* **62**, 149-160 (2007).

4 Fan, R., Olbricht, G., Baker, X. & Hou, C. Birth mass is the key to understanding the negative correlation between lifespan and body size in dogs. *Aging (Albany NY)* **8**, 3209-3222, doi:10.18632/aging.101081 (2016).

5 Tacutu, R. *et al.* Human Ageing Genomic Resources: integrated databases and tools for the biology and genetics of ageing. *Nucleic Acids Res* **41**, D1027-1033 (2013).

6 Fushan, A. A. *et al.* Gene expression defines natural changes in mammalian lifespan. *Aging Cell* **14**, 352-365, doi:10.1111/acel.12283 (2015).

7 Van Daele, P. A., Verheyen, E., Brunain, M. & Adriaens, D. Cytochrome b sequence analysis reveals differential molecular evolution in African mole-rats of the chromosomally hyperdiverse genus Fukomys (Bathyergidae, Rodentia) from the Zambezian region. *Mol Phylogenet Evol* **45**, 142-157, doi:10.1016/j.ympev.2007.04.008 (2007).

8 Gorbunova, V., Seluanov, A., Zhang, Z., Gladyshev, V. N. & Vijg, J. Comparative genetics of longevity and cancer: insights from long-lived rodents. *Nat Rev Genet* **15**, 531-540, doi:10.1038/nrg3728 (2014).

9 Jarvis, J. U. Eusociality in a mammal: cooperative breeding in naked mole-rat colonies. *Science* **212**, 571-573 (1981).

10 Buffenstein, R. Negligible senescence in the longest living rodent, the naked mole-rat: insights from a successfully aging species. *J Comp Physiol B* **178**, 439-445, doi:10.1007/s00360-007-0237-5 (2008).

11 Delaney, M. A. *et al.* Initial Case Reports of Cancer in Naked Mole-rats (Heterocephalus glaber). *Vet Pathol* **53**, 691-696, doi:10.1177/0300985816630796 (2016).

12 Taylor, K. R., Milone, N. A. & Rodriguez, C. E. Four Cases of Spontaneous Neoplasia in the Naked Mole-Rat (Heterocephalus glaber), A Putative Cancer-Resistant Species. *J Gerontol A Biol Sci Med Sci* **72**, 38-43, doi:10.1093/gerona/glw047 (2017).

13 Seluanov, A. *et al.* Hypersensitivity to contact inhibition provides a clue to cancer resistance of naked mole-rat. *Proc Natl Acad Sci U S A* **106**, 19352-19357, doi:10.1073/pnas.0905252106 (2009).

14 Gorbunova, V. *et al.* Cancer resistance in the blind mole rat is mediated by concerted necrotic cell death mechanism. *Proc Natl Acad Sci U S A* **109**, 19392-19396, doi:10.1073/pnas.1217211109 (2012).

15 Kosiol, C. *et al.* Patterns of positive selection in six Mammalian genomes. *PLoS Genet* **4**, e1000144 (2008).
16 Roux, J. *et al.* Patterns of positive selection in seven ant genomes. *Mol Biol Evol* **31**, 1661-1685 (2014).
17 Sahm, A., Bens, M., Platzer, M. & Cellerino, A. Parallel evolution of genes controlling mitonuclear balance in short-lived annual fishes. *Aging Cell*, doi:10.1111/acel.12577 (2017).
18 Kim, E. B. *et al.* Genome sequencing reveals insights into physiology and longevity of the naked mole rat. *Nature* **479**, 223-227 (2011).
19 Chandrasekaran, A., Idelchik, M. D. & Melendez, J. A. Redox control of senescence and age-related disease. *Redox Biol* **11**, 91-102, doi:10.1016/j.redox.2016.11.005 (2017).
20 Fang, X. *et al.* Genome-wide adaptive complexes to underground stresses in blind mole rats Spalax. *Nat Commun* **5**, 3966 (2014).
21 Davies, K. T., Bennett, N. C., Tsagkogeorga, G., Rossiter, S. J. & Faulkes, C. G. Family Wide Molecular Adaptations to Underground Life in African Mole-Rats Revealed by Phylogenomic Analysis. *Mol Biol Evol* **32**, 3089-3107 (2015).
22 Sahm, A., Platzer, M. & Cellerino, A. Outgroups and Positive Selection: The Nothobranchius furzeri Case. *Trends Genet* **32**, 523-525 (2016).
23 Fang, X. *et al.* Adaptations to a subterranean environment and longevity revealed by the analysis of mole rat genomes. *Cell Rep* **8**, 1354-1364 (2014).
24 Zhang, J., Nielsen, R. & Yang, Z. Evaluation of an improved branch-site likelihood method for detecting positive selection at the molecular level. *Mol Biol Evol* **22**, 2472-2479 (2005).
25 Bakewell, M. A., Shi, P. & Zhang, J. More genes underwent positive selection in chimpanzee evolution than in human evolution. *Proc Natl Acad Sci U S A* **104**, 7489-7494 (2007).
26 Gaya-Vidal, M. & Alba, M. M. Uncovering adaptive evolution in the human lineage. *BMC Genomics* **15**, 599 (2014).
27 Fletcher, W. & Yang, Z. The effect of insertions, deletions, and alignment errors on the branch-site test of positive selection. *Mol Biol Evol* **27**, 2257-2267 (2010).
28 Sahm, A., Bens, M., Platzer, M. & Szafranski, K. PosiGene: automated and easy-to-use pipeline for genome-wide detection of positively selected genes. *Nucleic Acids Res*, doi:10.1093/nar/gkx179 (2017).
29 Durlinger, A. L., Visser, J. A. & Themmen, A. P. Regulation of ovarian function: the role of anti-Mullerian hormone. *Reproduction* **124**, 601-609 (2002).
30 Semeiks, J. & Grishin, N. V. A method to find longevity-selected positions in the mammalian proteome. *PLoS One* **7**, e38595, doi:10.1371/journal.pone.0038595 (2012).
31 Hughes, K. A. & Reynolds, R. M. Evolutionary and mechanistic theories of aging. *Annu Rev Entomol* **50**, 421-445, doi:10.1146/annurev.ento.50.071803.130409 (2005).
32 Bartke, A. Healthy aging: is smaller better? - a mini-review. *Gerontology* **58**, 337-343, doi:10.1159/000335166 (2012).
33 Dai, H., Leeder, J. S. & Cui, Y. A modified generalized Fisher method for combining probabilities from dependent tests. *Front Genet* **5**, 32, doi:10.3389/fgene.2014.00032 (2014).
34 Blagosklonny, M. V. Aging: ROS or TOR. *Cell Cycle* **7**, 3344-3354, doi:10.4161/cc.7.21.6965 (2008).
35 Blagosklonny, M. V. Answering the ultimate question "what is the proximal cause of aging?". *Aging (Albany NY)* **4**, 861-877, doi:10.18632/aging.100525 (2012).
36 Licastro, F. *et al.* Innate immunity and inflammation in ageing: a key for understanding age-related diseases. *Immun Ageing* **2**, 8, doi:10.1186/1742-4933-2-8 (2005).
37 Pitt, J. N. & Kaeberlein, M. Why is aging conserved and what can we do about it? *PLoS Biol* **13**, e1002131, doi:10.1371/journal.pbio.1002131 (2015).
38 Chung, H. Y. *et al.* Molecular inflammation: underpinnings of aging and age-related diseases. *Ageing Res Rev* **8**, 18-30, doi:10.1016/j.arr.2008.07.002 (2009).
39 Johnson, S. C., Rabinovitch, P. S. & Kaeberlein, M. mTOR is a key modulator of ageing and age-related disease. *Nature* **493**, 338-345, doi:10.1038/nature11861 (2013).

40 Kenyon, C. J. The genetics of ageing. *Nature* **464**, 504-512, doi:10.1038/nature08980 (2010).

41 Jung, C. H., Ro, S. H., Cao, J., Otto, N. M. & Kim, D. H. mTOR regulation of autophagy. *FEBS Lett* **584**, 1287-1295, doi:10.1016/j.febslet.2010.01.017 (2010).

42 Rubinsztein, D. C., Marino, G. & Kroemer, G. Autophagy and aging. *Cell* **146**, 682-695, doi:10.1016/j.cell.2011.07.030 (2011).

43 Bandyopadhyay, U., Kaushik, S., Varticovski, L. & Cuervo, A. M. The chaperone-mediated autophagy receptor organizes in dynamic protein complexes at the lysosomal membrane. *Mol Cell Biol* **28**, 5747-5763, doi:10.1128/MCB.02070-07 (2008).

44 Cuervo, A. M. & Dice, J. F. A receptor for the selective uptake and degradation of proteins by lysosomes. *Science* **273**, 501-503 (1996).

45 Zhang, C. & Cuervo, A. M. Restoration of chaperone-mediated autophagy in aging liver improves cellular maintenance and hepatic function. *Nat Med* **14**, 959-965, doi:10.1038/nm.1851 (2008).

46 Kevei, E. & Hoppe, T. Ubiquitin sets the timer: impacts on aging and longevity. *Nat Struct Mol Biol* **21**, 290-292, doi:10.1038/nsmb.2806 (2014).

47 Saez, I. & Vilchez, D. The Mechanistic Links Between Proteasome Activity, Aging and Age-related Diseases. *Curr Genomics* **15**, 38-51, doi:10.2174/1389202915011403061133344 (2014).

48 Chondrogianni, N., Petropoulos, I., Franceschi, C., Friguet, B. & Gonos, E. S. Fibroblast cultures from healthy centenarians have an active proteasome. *Exp Gerontol* **35**, 721-728 (2000).

49 Lee, G. Y. *et al.* Comparative oncogenomics identifies PSMB4 and SHMT2 as potential cancer driver genes. *Cancer Res* **74**, 3114-3126, doi:10.1158/0008-5472.CAN-13-2683 (2014).

50 Beck, B. D. *et al.* Human Pso4 is a metnase (SETMAR)-binding partner that regulates metnase function in DNA repair. *J Biol Chem* **283**, 9023-9030, doi:10.1074/jbc.M800150200 (2008).

51 Zahn, J. M. *et al.* Transcriptional profiling of aging in human muscle reveals a common aging signature. *PLoS Genet* **2**, e115, doi:10.1371/journal.pgen.0020115.eor (2006).

52 Ori, A. *et al.* Integrated Transcriptome and Proteome Analyses Reveal Organ-Specific Proteome Deterioration in Old Rats. *Cell Syst* **1**, 224-237, doi:10.1016/j.cels.2015.08.012 (2015).

53 Reichwald, K. *et al.* Insights into Sex Chromosome Evolution and Aging from the Genome of a Short-Lived Fish. *Cell* **163**, 1527-1538 (2015).

54 Janssens, G. E. *et al.* Protein biogenesis machinery is a driver of replicative aging in yeast. *Elife* **4**, e08527, doi:10.7554/eLife.08527 (2015).

55 Baumgart, M. *et al.* Longitudinal RNA-Seq Analysis of Vertebrate Aging Identifies Mitochondrial Complex I as a Small-Molecule-Sensitive Modifier of Lifespan. *Cell Syst* **2**, 122-132, doi:10.1016/j.cels.2016.01.014 (2016).

56 Hansen, M. *et al.* Lifespan extension by conditions that inhibit translation in Caenorhabditis elegans. *Aging Cell* **6**, 95-110, doi:10.1111/j.1474-9726.2006.00267.x (2007).

57 Hofmann, J. W. *et al.* Reduced expression of MYC increases longevity and enhances healthspan. *Cell* **160**, 477-488, doi:10.1016/j.cell.2014.12.016 (2015).

58 Bratic, A. & Larsson, N. G. The role of mitochondria in aging. *J Clin Invest* **123**, 951-957, doi:10.1172/JCI64125 (2013).

59 Bonawitz, N. D., Chatenay-Lapointe, M., Pan, Y. & Shadel, G. S. Reduced TOR signaling extends chronological life span via increased respiration and upregulation of mitochondrial gene expression. *Cell Metab* **5**, 265-277, doi:10.1016/j.cmet.2007.02.009 (2007).

60 Schieke, S. M. *et al.* The mammalian target of rapamycin (mTOR) pathway regulates mitochondrial oxygen consumption and oxidative capacity. *J Biol Chem* **281**, 27643-27652, doi:10.1074/jbc.M603536200 (2006).

61 Miwa, S. *et al.* Low abundance of the matrix arm of complex I in mitochondria predicts longevity in mice. *Nat Commun* **5**, 3837, doi:10.1038/ncomms4837 (2014).

686 62 Dillin, A. *et al.* Rates of behavior and aging specified by mitochondrial function during
687 development. *Science* **298**, 2398-2401, doi:10.1126/science.1077780 (2002).
688 63 Balaban, R. S., Nemoto, S. & Finkel, T. Mitochondria, oxidants, and aging. *Cell* **120**, 483-495,
689 doi:10.1016/j.cell.2005.02.001 (2005).
690 64 Kim, G. H., Kim, J. E., Rhie, S. J. & Yoon, S. The Role of Oxidative Stress in Neurodegenerative
691 Diseases. *Exp Neurobiol* **24**, 325-340, doi:10.5607/en.2015.24.4.325 (2015).
692 65 Barja, G. The mitochondrial free radical theory of aging. *Prog Mol Biol Transl Sci* **127**, 1-27,
693 doi:10.1016/B978-0-12-394625-6.00001-5 (2014).
694 66 Umeda-Kameyama, Y. *et al.* Thioredoxin suppresses Parkin-associated endothelin receptor-
695 like receptor-induced neurotoxicity and extends longevity in Drosophila. *J Biol Chem* **282**,
696 11180-11187, doi:10.1074/jbc.M700937200 (2007).
697 67 Mitsui, A. *et al.* Overexpression of human thioredoxin in transgenic mice controls oxidative
698 stress and life span. *Antioxid Redox Signal* **4**, 693-696, doi:10.1089/15230860260220201
699 (2002).
700 68 Perez, V. I. *et al.* Thioredoxin 1 overexpression extends mainly the earlier part of life span in
701 mice. *J Gerontol A Biol Sci Med Sci* **66**, 1286-1299, doi:10.1093/gerona/glr125 (2011).
702 69 Flynn, J. M. & Melov, S. SOD2 in mitochondrial dysfunction and neurodegeneration. *Free*
703 *Radic Biol Med* **62**, 4-12, doi:10.1016/j.freeradbiomed.2013.05.027 (2013).
704 70 Son, M., Fu, Q., Puttaparthi, K., Matthews, C. M. & Elliott, J. L. Redox susceptibility of SOD1
705 mutants is associated with the differential response to CCS over-expression in vivo. *Neurobiol*
706 *Dis* **34**, 155-162 (2009).
707 71 Andziak, B. & Buffenstein, R. Disparate patterns of age-related changes in lipid peroxidation
708 in long-lived naked mole-rats and shorter-lived mice. *Aging Cell* **5**, 525-532,
709 doi:10.1111/j.1474-9726.2006.00246.x (2006).
710 72 Andziak, B., O'Connor, T. P. & Buffenstein, R. Antioxidants do not explain the disparate
711 longevity between mice and the longest-living rodent, the naked mole-rat. *Mech Ageing Dev*
712 **126**, 1206-1212, doi:10.1016/j.mad.2005.06.009 (2005).
713 73 Andziak, B. *et al.* High oxidative damage levels in the longest-living rodent, the naked mole-
714 rat. *Aging Cell* **5**, 463-471, doi:10.1111/j.1474-9726.2006.00237.x (2006).
715 74 Schmidt, C. M., Blount, J. D. & Bennett, N. C. Reproduction is associated with a tissue-
716 dependent reduction of oxidative stress in eusocial female Damaraland mole-rats (Fukomys
717 damarensis). *PLoS One* **9**, e103286, doi:10.1371/journal.pone.0103286 (2014).
718 75 Dammann, P. & Burda, H. Sexual activity and reproduction delay ageing in a mammal. *Curr*
719 *Biol* **16**, R117-118, doi:10.1016/j.cub.2006.02.012 (2006).
720 76 Dammann, P., Sumbera, R., Massmann, C., Scherag, A. & Burda, H. Extended longevity of
721 reproductives appears to be common in Fukomys mole-rats (Rodentia, Bathyergidae). *PLoS*
722 *One* **6**, e18757, doi:10.1371/journal.pone.0018757 (2011).
723 77 Schmidt, C. M., Bennett, N. C. & Jarvis, J. U. The long-lived queen: reproduction and longevity
724 in female eusocial Damaraland mole-rats (Fukomys damarensis). . *African Zoology* **48**, 193-
725 196 (2013).
726 78 Vistoli, G. *et al.* Advanced glycoxidation and lipoxidation end products (AGEs and ALEs): an
727 overview of their mechanisms of formation. *Free Radic Res* **47 Suppl 1**, 3-27,
728 doi:10.3109/10715762.2013.815348 (2013).
729 79 Simm, A. *et al.* Protein glycation - Between tissue aging and protection. *Exp Gerontol* **68**, 71-
730 75, doi:10.1016/j.exger.2014.12.013 (2015).
731 80 Dammann, P., Sell, D. R., Begall, S., Strauch, C. & Monnier, V. M. Advanced glycation end-
732 products as markers of aging and longevity in the long-lived Ansell's mole-rat (Fukomys
733 anselli). *J Gerontol A Biol Sci Med Sci* **67**, 573-583, doi:10.1093/gerona/glr208 (2012).
734 81 Helgadottir, A. *et al.* Variants with large effects on blood lipids and the role of cholesterol and
735 triglycerides in coronary disease. *Nat Genet* **48**, 634-639, doi:10.1038/ng.3561 (2016).

82 Mahley, R. W. Central Nervous System Lipoproteins: ApoE and Regulation of Cholesterol Metabolism. *Arterioscler Thromb Vasc Biol* **36**, 1305-1315, doi:10.1161/ATVBAHA.116.307023 (2016).

83 Broer, L. *et al.* GWAS of longevity in CHARGE consortium confirms APOE and FOXO3 candidacy. *J Gerontol A Biol Sci Med Sci* **70**, 110-118, doi:10.1093/gerona/glu166 (2015).

84 Macedo, M. F. & de Sousa, M. Transferrin and the transferrin receptor: of magic bullets and other concerns. *Inflamm Allergy Drug Targets* **7**, 41-52 (2008).

85 Hare, D., Ayton, S., Bush, A. & Lei, P. A delicate balance: Iron metabolism and diseases of the brain. *Front Aging Neurosci* **5**, 34, doi:10.3389/fnagi.2013.00034 (2013).

86 Jarvis, J. U. & Bennett, N. C. Eusociality has evolved independently in two genera of bathyergid mole-rats — but occurs in no other subterranean mammal. *Behavioral Ecology and Sociobiology* **33**, 253-260 (1993).

87 Burda, H., Honeycutt, R. L., Begall, S., Locker-Grütjen, O. & Scharff, A. Are naked and common mole-rats eusocial and if so, why? *Behavioral Ecology and Sociobiology* **47**, 293-303 (2000).

88 Sobrero, R., Inostroza-Michael, O., Hernandez, C. E. & Ebensperger, L. A. Phylogeny modulates the effects of ecological conditions on group living across hystricognath rodents. *Animal Behaviour* **94**, 27-34 (2014).

89 Smorkatcheva, A. V. & Lukhtanov, V. A. Evolutionary association between subterranean lifestyle and female sociality in rodents. *Mammalian Biology* **79**, 101-109 (2014).

90 Woodard, S. H. *et al.* Genes involved in convergent evolution of eusociality in bees. *Proc Natl Acad Sci U S A* **108**, 7472-7477, doi:10.1073/pnas.1103457108 (2011).

91 Malkki, H. Neurodevelopmental disorders: Impaired immune system function linked to social behaviour deficits in mice. *Nat Rev Neurol* **12**, 431, doi:10.1038/nrneurol.2016.109 (2016).

92 Estes, M. L. & McAllister, A. K. Immune mediators in the brain and peripheral tissues in autism spectrum disorder. *Nat Rev Neurosci* **16**, 469-486, doi:10.1038/nrn3978 (2015).

93 Nudel, R. *et al.* Associations of HLA alleles with specific language impairment. *J Neurodev Disord* **6**, 1, doi:10.1186/1866-1955-6-1 (2014).

94 Kodavali, C. V. *et al.* HLA associations in schizophrenia: are we re-discovering the wheel? *Am J Med Genet B Neuropsychiatr Genet* **165B**, 19-27, doi:10.1002/ajmg.b.32195 (2014).

95 Torres, A. R. *et al.* The association and linkage of the HLA-A2 class I allele with autism. *Hum Immunol* **67**, 346-351, doi:10.1016/j.humimm.2006.01.001 (2006).

96 Viljakainen, L. *et al.* Rapid evolution of immune proteins in social insects. *Mol Biol Evol* **26**, 1791-1801, doi:10.1093/molbev/msp086 (2009).

97 Guruharsha, K. G., Kankel, M. W. & Artavanis-Tsakonas, S. The Notch signalling system: recent insights into the complexity of a conserved pathway. *Nat Rev Genet* **13**, 654-666, doi:10.1038/nrg3272 (2012).

98 Duncan, E. J., Hyink, O. & Dearden, P. K. Notch signalling mediates reproductive constraint in the adult worker honeybee. *Nat Commun* **7**, 12427, doi:10.1038/ncomms12427 (2016).

99 Frick, C., Atanasov, A. G., Arnold, P., Ozols, J. & Odermatt, A. Appropriate function of 11beta-hydroxysteroid dehydrogenase type 1 in the endoplasmic reticulum lumen is dependent on its N-terminal region sharing similar topological determinants with 50-kDa esterase. *J Biol Chem* **279**, 31131-31138, doi:10.1074/jbc.M313666200 (2004).

100 Clarke, F. M. & Faulkes, C. G. Dominance and queen succession in captive colonies of the eusocial naked mole-rat, Heterocephalus glaber. *Proc Biol Sci* **264**, 993-1000, doi:10.1098/rspb.1997.0137 (1997).

101 Hawes, D. J., Brennan, J. & Dadds, M. R. Cortisol, callous-unemotional traits, and pathways to antisocial behavior. *Curr Opin Psychiatry* **22**, 357-362, doi:10.1097/YCO.0b013e32832bfa6d (2009).

102 Sanchez-Martin, J. R. *et al.* Social behavior, cortisol, and sIgA levels in preschool children. *J Psychosom Res* **50**, 221-227 (2001).

103 Holmes, M. C., Kotelevtsev, Y., Mullins, J. J. & Seckl, J. R. Phenotypic analysis of mice bearing targeted deletions of 11beta-hydroxysteroid dehydrogenases 1 and 2 genes. *Mol Cell Endocrinol* **171**, 15-20 (2001).

104 Anderson, A. & Walker, B. R. 11beta-HSD1 inhibitors for the treatment of type 2 diabetes and cardiovascular disease. *Drugs* **73**, 1385-1393, doi:10.1007/s40265-013-0112-5 (2013).

105 Fritz-Wolf, K., Kehr, S., Stumpf, M., Rahlfs, S. & Becker, K. Crystal structure of the human thioredoxin reductase-thioredoxin complex. *Nat Commun* **2**, 383, doi:10.1038/ncomms1382 (2011).

106 Weichsel, A., Gasdaska, J. R., Powis, G. & Montfort, W. R. Crystal structures of reduced, oxidized, and mutated human thioredoxins: evidence for a regulatory homodimer. *Structure* **4**, 735-751 (1996).

107 Hwang, J., Nguyen, L. T., Jeon, Y. H., Lee, C. Y. & Kim, M. H. Crystal structure of fully oxidized human thioredoxin. *Biochem Biophys Res Commun* **467**, 218-222, doi:10.1016/j.bbrc.2015.10.003 (2015).

108 Watson, W. H. *et al.* Redox potential of human thioredoxin 1 and identification of a second dithiol/disulfide motif. *J Biol Chem* **278**, 33408-33415, doi:10.1074/jbc.M211107200 (2003).

109 Hashemy, S. I. & Holmgren, A. Regulation of the catalytic activity and structure of human thioredoxin 1 via oxidation and S-nitrosylation of cysteine residues. *J Biol Chem* **283**, 21890-21898, doi:10.1074/jbc.M801047200 (2008).

110 Wu, C. *et al.* Thioredoxin 1-mediated post-translational modifications: reduction, transnitrosylation, denitrosylation, and related proteomics methodologies. *Antioxid Redox Signal* **15**, 2565-2604, doi:10.1089/ars.2010.3831 (2011).

111 Hall, D. R. *et al.* The crystal and molecular structures of diferric porcine and rabbit serum transferrins at resolutions of 2.15 and 2.60 A, respectively. *Acta Crystallogr D Biol Crystallogr* **58**, 70-80 (2002).

112 Medawar, P. B. An unsolved problem of biology. *(Printed lecture: University College London)* (1952).

113 Groenewoud, M. J. & Zwartkruis, F. J. Rheb and Rags come together at the lysosome to activate mTORC1. *Biochem Soc Trans* **41**, 951-955, doi:10.1042/BST20130037 (2013).

114 Bens, M. *et al.* FRAMA: from RNA-seq data to annotated mRNA assemblies. *BMC Genomics* **17**, 54, doi:10.1186/s12864-015-2349-8 (2016).

115 Stanke, M., Schoffmann, O., Morgenstern, B. & Waack, S. Gene prediction in eukaryotes with a generalized hidden Markov model that uses hints from external sources. *BMC Bioinformatics* **7**, 62, doi:10.1186/1471-2105-7-62 (2006).

116 Dobin, A. *et al.* STAR: ultrafast universal RNA-seq aligner. *Bioinformatics* **29**, 15-21, doi:10.1093/bioinformatics/bts635 (2013).

117 Kent, W. J. BLAT--the BLAST-like alignment tool. *Genome Res* **12**, 656-664, doi:10.1101/gr.229202. Article published online before March 2002 (2002).

118 Kapustin, Y., Souvorov, A., Tatusova, T. & Lipman, D. Splign: algorithms for computing spliced alignments with identification of paralogs. *Biol Direct* **3**, 20, doi:10.1186/1745-6150-3-20 (2008).

119 Li, H. & Durbin, R. Fast and accurate short read alignment with Burrows-Wheeler transform. *Bioinformatics* **25**, 1754-1760, doi:10.1093/bioinformatics/btp324 (2009).

120 Love, M. I., Huber, W. & Anders, S. Moderated estimation of fold change and dispersion for RNA-seq data with DESeq2. *Genome Biol* **15**, 550, doi:10.1186/s13059-014-0550-8 (2014).

121 Luo, W., Friedman, M. S., Shedden, K., Hankenson, K. D. & Woolf, P. J. GAGE: generally applicable gene set enrichment for pathway analysis. *BMC Bioinformatics* **10**, 161, doi:10.1186/1471-2105-10-161 (2009).

122 Supek, F., Bosnjak, M., Skunca, N. & Smuc, T. REVIGO summarizes and visualizes long lists of gene ontology terms. *PLoS One* **6**, e21800, doi:10.1371/journal.pone.0021800 (2011).

836 123 Arnold, K., Bordoli, L., Kopp, J. & Schwede, T. The SWISS-MODEL workspace: a web-based
837 environment for protein structure homology modelling. *Bioinformatics* **22**, 195-201,
838 doi:10.1093/bioinformatics/bti770 (2006).
839 124 Biasini, M. *et al.* SWISS-MODEL: modelling protein tertiary and quaternary structure using
840 evolutionary information. *Nucleic Acids Res* **42**, W252-258, doi:10.1093/nar/gku340 (2014).
841 125 Pettersen, E. F. *et al.* UCSF Chimera--a visualization system for exploratory research and
842 analysis. *J Comput Chem* **25**, 1605-1612, doi:10.1002/jcc.20084 (2004).

843 Acknowledgements

844 We thank Ivonne Görlich, Christiane Vole and Yoshiyuki Henning for excellent assistance, Debra Weih
845 for proofreading the manuscript and Christoph Kaether for helpful discussions. This work was funded
846 by the Deutsche Forschungsgemeinschaft (DFG, PL 173/8-1 and DA 992/3-1), the European
847 Community's Seventh Framework Programme (FP7-HEALTH-2012-279281) as well as the Leibniz
848 association (SAW-2012-FLI-2).

849 Author contributions

850 MP, PD and KS initiated the project. MP, AS and KS managed the project. PD, HB, TH, SH and MS
851 provided samples; MGr was in charge for the sequencing; MB and AS performed assemblies and gene
852 expression analyses; AS searched for PSGs; AS and HAK applied statistical tests; MGö performed
853 protein structure modeling; AS, MP, PD, AC, HB, CC and CM interpreted the data; AS, MP, PD, AC and
854 MGö wrote the manuscript. All authors read and approved the final manuscript.

855 Competing interests

856 The authors declare no competing financial interests.

857 Corresponding author

858 Correspondence to Arne Sahm (arne.sahm@fli-leibniz.de).

Supplementary information

Supplementary tables: S1-S24.xls

Table S1. Data Sources for assemblies and sequence statistics.

Table S2. Samples that were sequenced to create genome/transcriptome assemblies.

Table S3. PSGs on multiple branches.

Table S4. Overview of positively selected genes (FDR≤0.05) on examined branches.

Table S5. Results on branch 1.

Table S6. Results on branch 2.

Table S7. Results on branch 3.

Table S8. Results on branch 4.

Table S9. Results on branch 5.

Table S10. Results on branch 6.

Table S11. Results on branch 7.

Table S12. Results on branch 8.

Table S13. Results on branch 9.

Table S14. Results on branch 10.

Table S15. Results on branch 11.

Table S16. Overlaps between this and previos studies.

Table S17. Samples that were RNA-sequenced to examine gene regulation during aging.

878 Table S18. DESeq2 result for gene expression comparison of young (Ø 3.42 years) vs. old (>21 years)
879 naked mole-rats.

880 Table S19. DESeq2 result for gene expression comparison of young (6 months) vs. old (24 months)
881 rats.

882 Table S20. GAGE gene ontology enrichment for expression changes during NMR aging (Ø 3.42 vs > 21
883 years, FDR<=0.05, all down-regulated) .

884 Table S21. REVIGO treemap result of GAGE enrichment for differential expression during NMR aging.

885 Table S22. REVIGO representative categories (representative term given) of GAGE enrichment for
886 differential expression during NMR aging.

887 Table S23. PSGs in aging relevant summarized REVIGO categories and quadrant 1 (up-regulated in rat
888 and down-regulated in NMR).

889 Table S24. Gene ontologies enriched for PSGs on examined branches based on GOStats and Fisher's
890 exact test (FDR≤0.05).

891

892 **Supplement data:** ftp://genome.leibniz-fli.de/pub/mrps2017/supplement_data.tar.gz

893

894 The package contains visualizations of alignments and positively selected sites for all genes and
895 branches that were analyzed in this article.

896